Hindawi
Advances in Civil Engineering
Volume 2019, Article ID 2045125, 19 pages
https://doi.org/10.1155/2019/2045125

Research Article

Predictive Analysis of Settlement Risk in Tunnel Construction: A Bow-Tie-Bayesian Network Approach

Wen Liu,[1] **Shihong Zhai**,[2,3,4] **and Wenli Liu**[5]

[1]*Post-Doctoral, CCCC Second Harbor Engineering Co., Ltd., No. 11 Jinyin Lake Road, Dongxihu District, Wuhan 430074, China*
[2]*Professor-Level Senior Engineers, Key Laboratory of Large-Span Bridge Construction Technology for Transportation Industry, No. 11 Jinyin Lake Road, Dongxihu District, Wuhan 430074, China*
[3]*Professor-Level Senior Engineers, Research and Development Center of Transportation Industry of Intelligent Manufacturing Technologies of Transport Infrastructure, No. 11 Jinyin Lake Road, Dongxihu District, Wuhan 430074, China*
[4]*Professor-Level Senior Engineers, CCCC Highway Bridges National Engineering Research Centre Co., Ltd., No. 11 Jinyin Lake Road, Dongxihu District, Wuhan 430074, China*
[5]*Postdoctoral Research Fellow, School of Civil Engineering & Mechanics, Huazhong University of Science and Technology, Hubei, Wuhan 430074, China*

Correspondence should be addressed to Wenli Liu; newheny2014@hotmail.com

Received 18 January 2019; Accepted 23 June 2019; Published 10 July 2019

Academic Editor: Dong Zhao

A hybrid method consisting of bow-tie-Bayesian network (BT-BN) analysis and fuzzy theory is proposed in this research, in order to support predictive analysis of settlement risk during shield tunnel excavation. We verified the method by running a probabilistic safety assessment (PSA) for a tunnel section in the Wuhan metro system. Firstly, we defined the "normal excavation phase" based on the fuzzy statistical test theory. We eliminated the noise records in the tunnel construction log and extracted the occurrence probability of facility failures from the denoised database. We then obtained the occurrence probability of environmental failures, operational errors, and multiple failures via aggregation of weighted expert opinions. The expert opinions were collected in the form of fuzzy numbers, including triangular numbers and trapezoidal numbers. Afterwards, we performed the BT-BN analysis. We mapped the bow-tie analysis to the Bayesian network and built a causal network PSA model consisting of 16 nodes. Causes of the excessive surface settlement and the resulting surface collapse were determined by bow-tie analysis. The key nodes of accidents were determined by introducing three key measures into the Bayesian inference. Finally, we described the safety measures for the key nodes based on the PSA results. These safety measures were capable of reducing the failure occurrence probability (in one year) of excessive surface settlement by 66%, thus lowering the accident probability caused by excessive surface settlement.

1. Introduction

There are intrinsic risks associated with shield tunnel excavation because of the limited knowledge about the existing subsurface conditions [1, 2]. Although the majority of shield tunnel construction projects have been completed safely, the surface collapse caused by excessive surface settlement did occur in several tunneling projects which resulted in major damage, injury, and loss of life. The worst accident of metro construction in China took place on November 15, 2008, in Hangzhou [3]. A massive cave-in during the construction of Metro Line 1 near the Xianghu station caused 21 injuries and 24 deaths, and the direct economic loss amounted to 49.61 million Yuan. A more recent accident took place on May 14, 2017, in Nanchang [4]. Excessive surface settlement during the construction of Metro Line 2 near the Bayi square station caused a cave-in more than 10 m in diameter and led to severe property losses. Therefore, it is imperative to systematically assess and manage the safety risks associated with shield tunnel excavation.

Traditionally, surface settlement in shield tunnel excavation has been studied both empirically and analytically.

A number of empirical formulae have been proposed based on extensive experiments and construction practices. Peck proposed in his classic formula that the surface settlement trough could be described by a normal distribution [5]. Since then, the Peck formula had been further improved and modified by many scholars, including Attewell et al. [6] and Rankin [7]. Attewell and Woodman proposed the cumulative probability curve [8]. O'Reilly and New suggested a predictive formula to estimate trough width, formation loss, and surface settlement [9]. Mair et al. and coworkers established their formula to calculate subsurface formation displacement [10]. Empirical formulae are widely used in practical engineering because of their simplicity, but their use is limited to crude estimations of the surface settlement because they are not accurate enough.

In contrast, analytical methods make reasonable simplifications of rock and soil to consider them as a medium with certain physical and mechanical properties and then derive the surface settlement via well-established mathematical models and mechanical theories [1]. The stochastic medium theory considered rock and soil as a "stochastic medium" and regards the surface settlement caused by tunnel excavation as a stochastic process [11–13]. Numerical analysis integrates the elastic-viscoplastic theory into numerical calculations and reduces the dimension of the calculations with discrete interpolation and analytic functions [14–16]. The primary problem with analytical methods is an oversimplification. In most cases, the task is reduced to solving the plane strain that is uniform, isotropic, and axisymmetric, although the practical situation in engineering and the geological formation at the construction site are much more complicated. In order to address those issues, artificial intelligence (AI) methods provide possible solutions, which have been exploited in studying the risk evolution of surface settlement.

This study aims to (1) clearly define the "normal excavation phase" of shield tunneling based on the fuzzy statistical test theory and extract the occurrence probability of facility failures from existing structured data; (2) in the absence of available data, determine the occurrence probability of environmental failure, operational error, and multiple failures by aggregating fuzzy numbers (triangular numbers and trapezoidal numbers) of expert opinion; (3) perform probabilistic safety assessment (PSA) of settlement failure in tunnel construction through bow-tie-Bayesian network (BT-BN) analysis; (4) identify the key nodes for excessive surface settlement-caused surface collapse; and (5) develop appropriate safety measures.

In this research, we examined the tunneling log of the Xiaodongmen-Wuchang section (XWS) during the construction of Metro Line 7 at Wuhan (Figure 1). Data were collected from XWS, and the key nodes that could cause cave-in due to the excessive surface settlement were extracted. We proposed safety measures that targeted the key nodes to reduce the likelihood of accidents. The XWS went from south to north, mainly along the Zhongshan road. The left tunnel was 1115.208 m in length and was excavated with a tunnel boring machine (TBM). The right tunnel was 1107.169 m in length and was excavated with a Komatsu tunnel boring machine. Both tunnels were excavated by using the earth pressure balance TBM. The minimum horizontal curve radius of the section was 400 m, and the line spacing was 12.6–50.5 m. The minimum longitudinal curve radius of the section was 3000 m. The section adopted a concave slope with the overlying soil of 10.5–45.4 m in thickness. Figure 1 shows a picture taken during the excavation of the XWS.

This paper is organized as follows. Section 2 presents the existing knowledge on the definitions of surface settlement incurred by shield tunnel excavation, classifies existing research methods on surface settlement in metro construction, and introduces the dynamic safety analysis of the BT-BN methodology. Section 3 defines the "normal excavation phase" of shield tunneling and presents the detailed procedures in carrying out the fuzzy BT-BN analysis. Section 4 examines the normal tunnel excavation in detail and applies the proposed fuzzy BT-BN method to the PSA analysis of excessive surface settlement-caused surface collapse in the XWS of Wuhan metro system. The conclusions and future works are drawn in Section 5.

2. Literature Review

2.1. Surface Settlement in Tunnel Construction. Surface settlement caused by shield tunnel excavation is a three-dimensional spatial process that involves the transformation, displacement response, and changing mechanical properties of different soil. As an approximation, an area of surface settlement can be seen to be developing as the TBM advances. The size of the area and the severity of settlement need to be determined to evaluate the spatial distribution of the surface settlement. Many countries have set out standards and benchmarks to monitor surface settlement during shield tunnel excavation (Table 1). Based on the Chinese standard GB 50911-2013 "Code for monitoring measurement of urban rail transit engineering" [17] as well as the standards of other countries, in this work, we classified risk levels of the surface settlement for the soft soil in the XWS as shown in Table 2.

In recent years, the artificial intelligence methods have been exploited in studying the risk evolution of surface settlement. Suwansawat and Einstein used artificial neural network (ANN) to evaluate the safety risks due to surface settlement in tunnel excavation by using the earth pressure balance TBM [18]. They took various influence factors as the inputs to their ANNs and predicted the surface settlement. Sun et al. introduced the theories and techniques of both artificial intelligence and automatic control into geotechnical engineering [19]. Specifically, an ANN model called "multistep circulation" was adopted for predicting the safety risk of surface settlement in shield tunneling. Fuzzy logic control was also applied to enable active safety control of deformation displacement in real time. However, existing artificial intelligence methods cannot analyze the key nodes with regard to surface settlement in shield tunnel excavation.

Figure 1: Location of XWS in the Wuhan metro system.

Table 1: Standards for monitoring surface settlement in shield tunnel excavation.

Country	U.S.	Japan	France	Germany	China
Acceptable surface settlement (mm)	10–15	25–50	Hard rock: 10–20 Soft rock: 20–50	50	Hard soil: 10–40 Soft soil: 15–45

Table 2: Classification of risk levels.

Level	1	2	3	4	5
Description	Negligible	Alarming	Serious	Dangerous	Catastrophic
Surface settlement (mm)	0–10	5–15	10–25	20–35	30–45

Besides, long learning time is needed and the requirement on known parameters can be demanding.

Overall, surface settlement in shield tunneling arises from various risk factors that involve geology, construction method, environment, and management. In order to thoroughly study the safety risk of surface settlement, it is necessary to analyze in real time the uncertain information in the risk factors from multiple sources. However, such uncertainty, including fuzziness and stochasticity, is ubiquitous and restricts the application of traditional methodologies such as empirical formula, simulation, and analytical modeling. Other methods based on artificial intelligence such as neural networks also suffer from the memory effect because it is difficult to update the risk factors in real time when new information arises.

2.2. Bayesian Network and Bow-Tie. In recent years, the bow-tie (BT) model has been combined with the Bayesian network (BN) to tackle various problems in which uncertainty is deeply rooted. The BT-BN approach has a solid foundation in mathematical theory and has unique advantages in dealing with complex dynamic uncertainty. It has been considered as an ideal tool for knowledge representation, inference, and forecasting in an uncertain environment.

Bow-tie analysis is a quantitative model that consists of fault tree (FT) analysis and event tree (ET) analysis [20] and allows investigating the causes and consequences of a given undesirable event. Cherubin et al. applied BT analysis as a simple and effective quantitative risk assessment (QRA) approach for the identification and evaluation of potential

hazards and associated risks with the baseline risk assessment tool (BART) [21]. Targoutzidis argued that BT analysis is an effective tool for identifying environmental risk sources because it can clearly show the connections between the cause, the loss events (LEs), the conditional events (CEs), and the outcome events (OEs) [22]. The BT approach has been applied in the risk assessment of hexane distillation, the risk management of harbor and maritime terminals, and the risk assessment of airworthiness in military aviation [23–25].

The focus of these BT models is to depict the entire scenario of the accident to identify and evaluate the potential causes and consequences but does not readily reveal the actual causes through logical connections and occurrence probability. This caveat can be remedied by mapping BT to BN. For example, Badreddine and Amor improved the BT model by exploiting the advantages of BN dynamic analysis. They built the BT chart in an automated and dynamic way to implement appropriate barriers to prevention and protection in dynamic systems [26]. Khakzad et al. made a dynamic risk analysis of systems whose physical reliability is updated periodically [27]. They made use of the Bayes theorem to periodically update the failure probability of safety barriers in the BT chart and estimated the probability of consequences based on the enhanced BT chart. It was argued that mapping BT to BN [28] could alleviate the limitations of BT caused by static factors. Abimbola et al. used BT and BN to determine the key factors of the integrity model. In their study, the posterior probability was obtained through the Bayes theorem, and the key factors were determined by the ratio of the posterior probability to the prior probability [29].

In summary, mapping BT to BN allows dynamic risk analysis, and the key factors of the system can be identified by calculating the posterior probability through the Bayes theorem. Meanwhile, since the conditional probability can be calculated via the Bayes theorem, the importance measure of PSA can also be introduced [30], and BN can be fitted with these important measures very well to calculate the importance measures accurately and easily. Therefore, the BT-BN analysis can not only analyze surface collapse caused by excessive surface settlement in shield tunneling metro construction but also use PSA to confirm the critical causes of accidents by adding the importance measures.

3. Methodology

BT analysis is used to display the scenario of the loss event (LE) in the system. In the BT model, the FT analysis can reveal the cause of the LE, and the consequences of LE can be determined by the ET analysis. In the proposed BT-BN method, the FT and ET analyses in the BT model are mapped to the BN such that the nodes that give rise to accidents can be more easily determined. The BT-BN method requires explicit occurrence probability of failure. Data for the failure probability of the TBM were extracted from construction log during the "normal excavation phase" of the XWS. When existing data could not provide the required information, expert opinion in the form of the fuzzy number was used to determine the corresponding failure probability. The consequences were then predicted by the BT-BN analysis, and the critical nodes related to the consequences were obtained. Figure 2 shows the flowchart of the proposed methodology.

3.1. "Normal Excavation Phase" of TBM

3.1.1. Fuzzy Statistical Test Theory. The concept of "fuzzy set," introduced by Zadeh, is a crucial extension of the classic set theory of Cantor [31]. The fuzzy set theory has matured over the past years to a well-established research area in mathematics and has found extensive applications in many fields. The fuzzy set A on domain X is, in fact, a function of $X \longrightarrow [0,1]$. The primary task of dealing with fuzziness in practical applications is to determine the membership function $A(x)$. Just like probabilistic theory cannot give precise but only approximate probability, due to limited knowledge and information, the fuzzy set theory can only establish the approximate degree of membership and consequently an estimated membership function. Fuzzy statistical tests that demonstrate the stability of frequency can be carried out to characterize the objectivity of degree of membership and to derive an approximate membership function.

Two-phase fuzzy statistics divides the domain X (e.g., TBM excavation speed) into two statistical sets, i.e., A ("normal") and A^c ("abnormal"). That is, two opposite fuzzy concepts compete for statistics in domain X. The so-called "two-phase" indicates $P_2 = \{A, A^c\}$ [32], i.e., each fuzzy test will establish a mapping e: $X \longrightarrow P_2$. This mapping divides the domain X, i.e., $\forall x \in X$, $A(x) + A^c(x) = 1$. The two-phase fuzzy statistical test contains four elements: (1) domain X; (2) a fixed element x_0 in X; (3) a varying classical set A^* in X (A^* reflects the flexible boundary of the fuzzy set A and allows to determine if the x_0 in each test conforms to the fuzzy concept described by A); and (4) condition S, which restricts the changes of A^*.

In fuzzy statistical tests, x_0 remains fixed while A^* is varied. In each test, a decision must be made as for whether x_0 belongs to A^*. Note that the changing A^* is always a subset of X. After n tests, the membership frequency of x_0 belonging to the fuzzy set A^* is calculated as $l_n(A)(x_0)$:

$$l_n(A)(x_0) = \frac{\text{number of times that "}x_0 \in A^*\text{"}}{n}. \quad (1)$$

It has been experimentally found that $l_n(A)(x_0)$ tends to stabilize as n increases. The stabilized value is referred to as the degree of membership that x_0 belongs to A:

$$l_n(A)(x_0) = \lim_{x \longrightarrow \infty} \frac{\text{number of times that "}x_0 \in A^*\text{"}}{n}. \quad (2)$$

3.1.2. Fuzzy Statistical Test of the Excavation Speed of TBM. Excavation speed is a macroscopic measure of the working state of the TBM. Therefore, the normal state of the TBM is characterized by the normal excavation speed. In our case, the normal excavation speed during tunneling was obtained by running a fuzzy statistical test with the construction logs of the XWS.

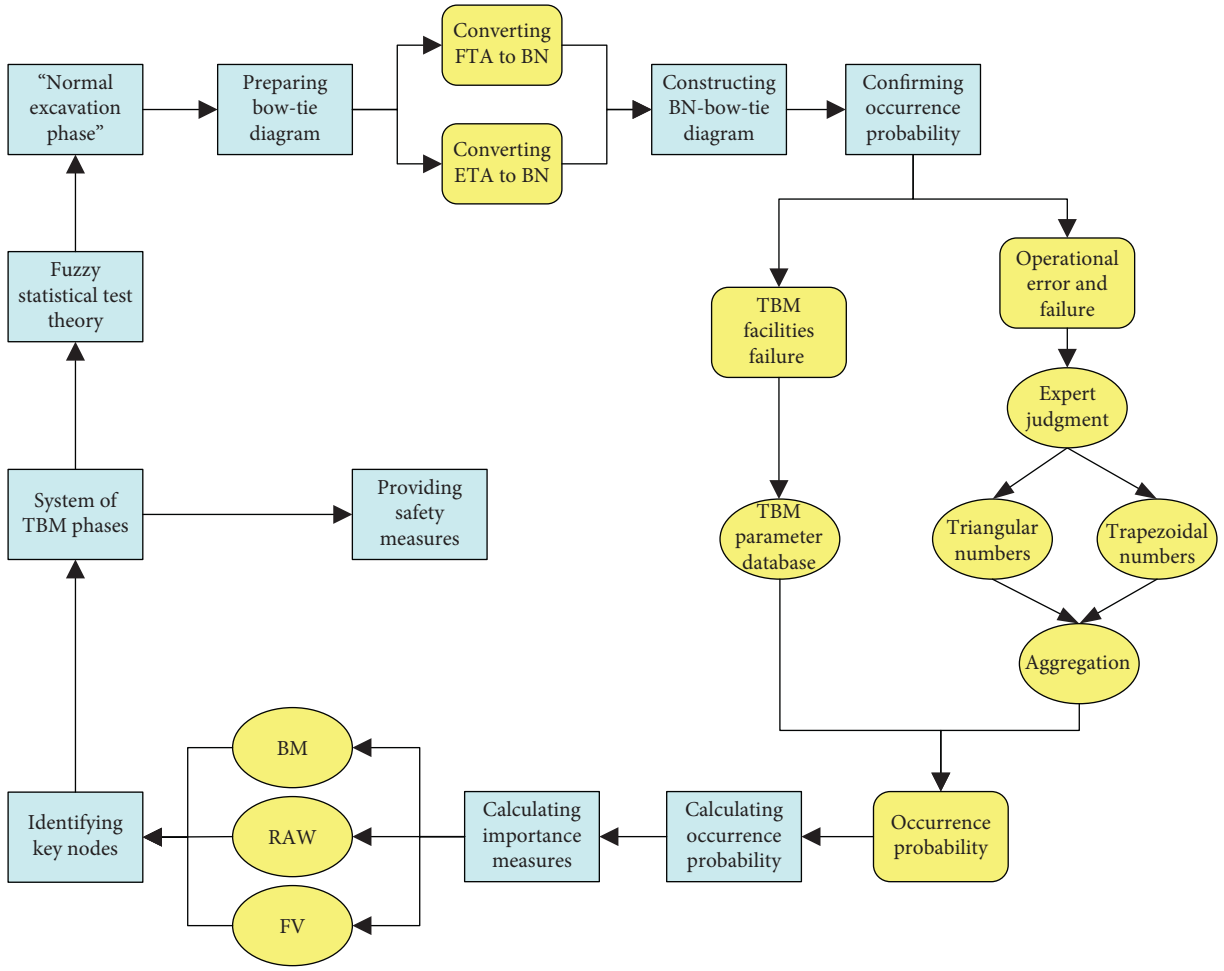

Figure 2: Flowchart of the proposed methodology.

In this work, the excavation speed of the TBM had a domain of $V = [1, 96]$ (mm/min). The fuzzy set A represents the fuzzy concept of "normal excavation speed." For the purpose of illustration, select an arbitrary excavation speed $v_0 = 23$ mm/min. Fuzzy statistical tests were then applied to determine the degree of membership that v_0 belonged to A. For the construction project at the XWS, the appropriate project logs over $n = 179$ days (715 segment rings for left and right tunnels) were selected. The appropriate logs excluded abnormal engineering situations (restrictive condition S) such as TBM launching, TBM arrival, and abnormal downtime, during which the formation was reinforced and the excavation speed could not be considered normal. In this way, the boundaries for the daily "normal excavation speed" could be determined for the left and right tunnels of the XWS (Table 3; Figure 3).

Table 4 shows the membership frequency that $v_0 = 23$ mm/min belonged to the normal excavation speed, as was determined by the statistical tests. Figure 4 shows that the membership frequency f that $v_0 = 23$ mm/min falls within the "normal excavation speed" of the TBM stabilized around 0.66. Hence, $A(v_0) = A(23) = 0.66$. The membership frequency f of other excavation speeds could also be obtained similarly. The data from the construction logs recorded a minimum and maximum excavation speed of 2 mm/min and 96 mm/min, respectively. Hence, we divided the domain V into 96 intervals each spanning 1 mm/min, starting from 1.5 mm/min and ending at 96.5 mm/min. The mean of each interval was used to calculate the membership frequency, and the results are shown in Table 5. A program was developed in MATLAB to reduce the computational complexity and save time.

Figure 5 plots the histogram of membership frequency based on the data in Table 5. The fitted curve of the membership function $A(v)$ was then drawn accordingly. The fitted curve conformed to the Cauchy distribution and could be expressed as follows:

$$\widetilde{A}(v) = \left\{ v, A(v) \mid A(v) = \left(1 + \left(\frac{v - 32}{12}\right)^2\right)^{-1}, \quad v \in N \right\}. \tag{3}$$

(1) Determination of the Standard Excavation Speed. In the fuzzy set theory [31], the element with the membership frequency $A(v) = 1$ is designated as the kernel of the fuzzy set A and written as "ker$A$." Figure 5 shows that ker$A = \{32\}$, i.e., $v_0 = 32$ mm/min, was the kernel of the fuzzy set of "normal excavation speed." Therefore, $v_0 = 32$ mm/min was considered as the standard excavation speed in the ensuing PSA analysis.

Table 3: Partial construction log of the "normal excavation speed" in the XWS.

$n = 1–10$	$n = 11–20$	$n = 21–30$	$n = 31–40$	$n = 41–50$	$n = 51–60$	$n = 61–70$	$n = 71–80$	$n = 81–90$	$n = 91–100$
30.3–50.6	25–32	27.6–42.4	7.8–42.5	25–35	18–39	27–43	20–41	30–47	20–54
32.4–38.8	26–34	23.2–47.6	8.3–41.7	28–46	20–35	24–40	10–40	30–61	32–63
28.4–39.6	27–42	23.3–44.5	20.2–47.6	17–35	15–42	27–47	20–35	20–61	32–58
30.3–38.8	23–36	20.5–42.7	24.2–42.5	28–37	27–41	20–33	17–32	30–60	20–37
30.3–36.3	12.3–34.8	28.2–45.6	28.7–52.6	17–36	21–37	22–34	8–40	14–58	24–40
32–44	17.8–32.5	18.2–42.6	19–32	20–37	31–41	27–48	8–40	27–74	25–48
31–42	19.8–37.4	13.7–37.5	22–45	20–35	30–40	30–42	20–50	15–55	24–51
31–39	13.5–32.6	15.6–32.6	21–44	21–37	30–35	25–43	20–50	25–45	32–46
30–42	13.4–32.6	20–37	19–42	20–35	20–40	28–36	20–46	28–52	25–40
31–38	15.6–36.4	15–40	20–41	20–37	25–40	22.5–37	31–42	31–47	20–35

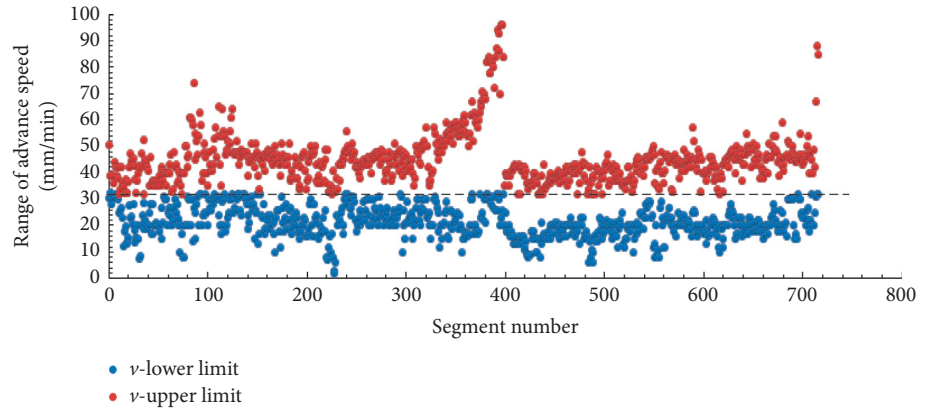

Figure 3: Distribution of the "normal excavation speed."

Table 4: Membership frequency of 23 mm/min belonging to the "normal excavation speed."

Description	Number and membership						
Number of rings	50	100	150	200	250	300	350
Membership counts	28	51	60	97	128	153	178
Membership frequency	0.56	0.51	0.4	0.49	0.51	0.51	0.51
Number of rings	400	450	500	550	600	650	715
Membership count	202	252	302	342	382	427	470
Membership frequency	0.51	0.56	0.61	0.62	0.64	0.66	0.66

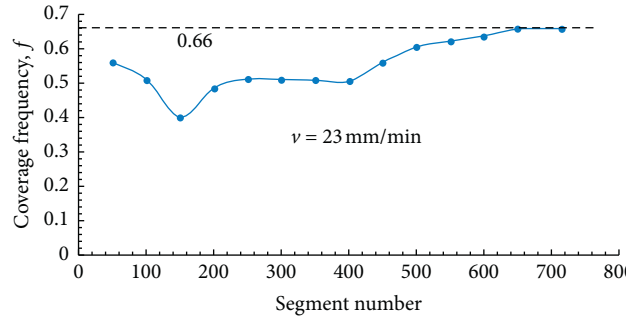

Figure 4: Membership frequency of 23 mm/min belonging to the "normal excavation speed."

(2) Determination of the Range of Excavation Speed. In the fuzzy set theory, all elements whose membership frequency $A(v) > 0$ constitute a support of the fuzzy set A and is written as "supp A," and all elements whose membership frequency $A(v) > \alpha$ is designated as the α cut set of the fuzzy set A and written as A_α. Figure 5 shows that the excavation speed fluctuated around the kernel (32 mm/min) during shield tunnel excavation. In order to express the range of normal excavation speed, the confidence level $\alpha = 0.5$ was selected and the excavation speed whose membership frequency satisfied $A(v) > 0.5$ was considered to constitute the interval of normal excavation speed (i.e., the 0.5 cut set of A).

Table 5: Membership frequency of the "normal excavation speed."

No.	Group	Count	Frequency
1	1.5–2.5	1	0.001
2	2.5–3.5	2	0.003
3	3.5–4.5	2	0.003
4	4.5–5.5	2	0.003
5	5.5–6.5	5	0.007
6	6.5–7.5	6	0.008
7	7.5–8.5	17	0.024
8	8.5–9.5	21	0.029
9	9.5–10.5	31	0.043
10	10.5–11.5	34	0.048
11	11.5–12.5	46	0.064
12	12.5–13.5	60	0.084
13	13.5–14.5	66	0.092
14	14.5–15.5	100	0.14
15	15.5–16.5	132	0.185
16	16.5–17.5	168	0.235
17	17.5–18.5	217	0.303
18	18.5–19.5	240	0.336
19	19.5–20.5	366	0.512
20	20.5–21.5	396	0.554
21	21.5–22.5	425	0.594
22	22.5–23.5	470	0.657
23	23.5–24.5	500	0.699
24	24.5–25.5	535	0.748
25	25.5–26.5	563	0.787
26	26.5–27.5	588	0.822
27	27.5–28.5	609	0.852
28	28.5–29.5	619	0.866
29	29.5–30.5	668	0.934
30	30.5–31.5	686	0.959
31	31.5–32.5	715	1
32	32.5–33.5	698	0.976
33	33.5–34.5	685	0.958
34	34.5–35.5	670	0.937
35	35.5–36.5	643	0.899
36	36.5–37.5	623	0.871
37	37.5–38.5	586	0.82
38	38.5–39.5	562	0.786
39	39.5–40.5	536	0.75
40	40.5–41.5	495	0.692
41	41.5–42.5	456	0.638
42	42.5–43.5	406	0.568
43	43.5–44.5	358	0.501
44	44.5–45.5	332	0.464
45	45.5–46.5	290	0.406
46	46.5–47.5	246	0.344
47	47.5–48.5	201	0.281
48	48.5–49.5	157	0.22
49	49.5–50.5	136	0.19
50	50.5–51.5	116	0.162
51	51.5–52.5	101	0.141
52	52.5–53.5	91	0.127
53	53.5–54.5	88	0.123
54	54.5–55.5	77	0.108
55	55.5–56.5	69	0.097
56	56.5–57.5	62	0.087
57	57.5–58.5	56	0.078
58	58.5–59.5	51	0.071
59	59.5–60.5	45	0.063
60	60.5–61.5	41	0.057
61	61.5–62.5	38	0.053
62	62.5–63.5	35	0.049
63	63.5–64.5	32	0.045
64	64.5–65.5	30	0.042
65	66.5–67.5	28	0.039
66	67.5–68.5	28	0.039
67	68.5–69.5	25	0.035
68	69.5–70.5	23	0.032
69	70.5–71.5	23	0.032
70	71.5–72.5	21	0.029
71	72.5–73.5	20	0.028
72	73.5–74.5	19	0.027
73	74.5–75.5	19	0.027
74	75.5–76.5	18	0.025
75	76.5–77.5	18	0.025
76	77.5–78.5	18	0.025
77	78.5–79.5	18	0.025
78	79.5–80.5	16	0.022
79	80.5–81.5	16	0.022
80	81.5–82.5	15	0.021
81	82.5–83.5	15	0.021
82	83.5–84.5	12	0.017
83	84.5–85.5	11	0.015
84	85.5–86.5	8	0.011
85	86.5–87.5	7	0.01
86	87.5–88.5	6	0.008
87	88.5–89.5	5	0.007
88	89.5–90.5	4	0.006
89	90.5–91.5	4	0.006
90	91.5–92.5	4	0.006
91	92.5–93.5	4	0.006
92	93.5–94.5	4	0.006
93	94.5–95.5	3	0.004
94	95.5–96.5	2	0.003
95	96.5–97.5	2	0.003

The set of normal excavation speed in Zadeh's form was ordered, as shown in equations (4) and (5). Thus, $v_0 = 20$–44 mm/min was considered as the range of normal excavation speed in the ensuing PSA analysis:

$$\begin{aligned}\widetilde{A}(v) = {} & \frac{0.50}{20} + \frac{0.54}{21} + \frac{0.59}{22} + \frac{0.64}{23} + \frac{0.69}{24} + \frac{0.75}{25} + \frac{0.80}{26} \\ & + \frac{0.85}{27} + \frac{0.90}{28} + \frac{0.94}{29} + \frac{0.97}{30} + \frac{0.99}{31} + \frac{1}{32} + \frac{0.99}{33} \\ & + \frac{0.97}{34} + \frac{0.94}{35} + \frac{0.90}{36} + \frac{0.85}{37} + \frac{0.80}{38} + \frac{0.75}{39} + \frac{0.69}{40} \\ & + \frac{0.64}{41} + \frac{0.59}{42} + \frac{0.54}{43} + \frac{0.50}{44},\end{aligned} \tag{4}$$

$$\begin{aligned}\operatorname{supp} \widetilde{A}(v) = \{ & 20, 21, 22, 23, 24, 25, 26, 27, 28, 29, 30, 31, 32, \\ & 33, 34, 35, 36, 37, 38, 39, 40, 41, 42, 43, 44\}.\end{aligned} \tag{5}$$

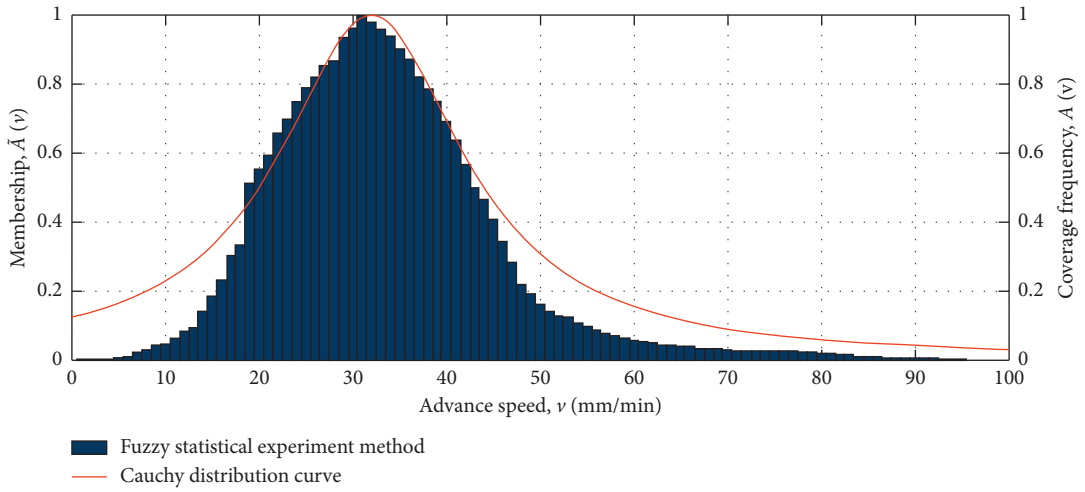

Figure 5: The histogram of membership frequency and the membership function of TBM excavation speed.

3.1.3. Fuzzy Statistical Tests of Excavation Parameters. The excavation speed of the TBM reflects the influence exerted by the excavation parameters (e.g., total thrust, face pressure, and cutter head torque) on the force and displacement of the surrounding soil. Therefore, it is necessary to determine the realistic and practical excavation parameters based on the excavation speed.

Formation reinforcement during TBM launching and TBM arrival can exert a strong influence on the shield tunnel excavation and lead to highly discrete parameters. Therefore, the data from the TBM launching and TBM arrival stages were discarded in studying the relationship between excavation speed and TBM parameters. Figure 6 shows how the TBM parameters varied with the excavation speed during the construction of the 715 segments in the XWS. The curves were fitted via MATLAB, and the slope of the curves was highly indicative of the correlation between the TBM parameters and the excavation speed.

In Figure 6(a), the total thrust (F) increased with rising excavation speed. This was because bentonite was used as a lubricant and injected around the shield of the TBM during excavation to reduce friction. When the amount of injected bentonite was appropriate, the friction coefficient between the shield and the surrounding soil would decrease, and the excavation speed would then increase when the thrust (F) was higher. In Figure 6(b), the excavation speed decreased when the cutter head torque (M_T) increased. This was because when the soil body of the tunneling face was relatively difficult to cut, a larger torque of the cutter head would be needed and the excavation speed would decrease. Figure 6(c) shows that during normal excavation, the pressure of the tunneling face increased slightly with rising excavation speed. Besides, Mair pointed out that during segment assembly, the downtime of TBM would decrease the soil and water pressure on the tunneling face, which could reduce the control pressure of the tunneling face [33]. The same pattern was observed in the current construction logs, and the R^2 value of the curve in Figure 6(c) was hence relatively low. Figure 6(d) shows that the grouting pressure decreased slightly with rising excavation speed. However, since the pressure of primary grouting was read off from the grouting pressure pump, the actual grouting pressure exerted on the surrounding soil was smaller, and the primary grouting pressure hence had limited impact on excavation speed.

(1) Determination of Standard TBM Parameters. It was determined from the fuzzy statistical tests above that the standard excavation speed was 32 mm/min. The corresponding standard TBM parameters could be determined accordingly from the following equation:

$$\mathrm{TBMP}_{\text{standard value}} = \frac{\sum_{n=1}^{N} \mathrm{TBMP}_{n,v}}{N}\Big|_{v=32}, \tag{6}$$

where TBMP is the TBM parameter and v is the excavation speed (mm/min).

(2) Determination of the Range of TBM Parameters. It was determined from the fuzzy statistical tests above that the range of excavation speed was 20–44 mm/min. The corresponding boundaries of TBM parameters could be determined from the extreme values in the monitoring records (Figure 6) via the following equation:

$$\begin{aligned} \mathrm{TBMP}_{\text{upper limit}} &= \max\left\{\mathrm{TBMP}_v\big|_{20\le v\le 44}\right\}, \\ \mathrm{TBMP}_{\text{lower limit}} &= \min\left\{\mathrm{TBMP}_v\big|_{20\le v\le 44}\right\}. \end{aligned} \tag{7}$$

(3) "Normal Excavation Phase" of TBM. According to the fuzzy set theory, the excavation speed in the "normal excavation phase" fell within 20–44 mm/min. The TBM was considered to be in the "normal excavation phase" when the excavation speed and the TBM parameters all fell within the prescribed ranges specified above and listed again in Table 6. The standard values and ranges were used further in the subsequent PSA analysis. Table 6 shows that among the examined parameters, the face pressure had a deviation interval of merely 19.6% and was controlled the

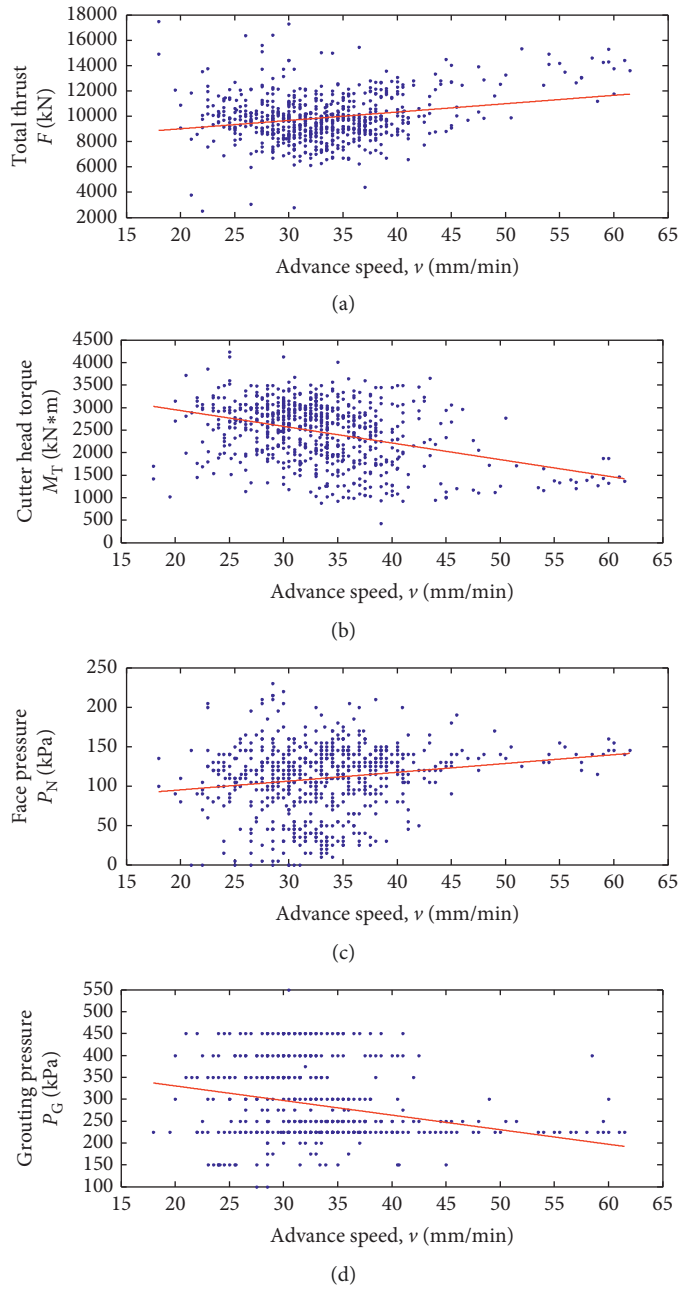

Figure 6: Variations in the TBM parameters at different excavation speeds (data from XW section): (a) total thrust versus excavation speed; (b) cutter head torque versus excavation speed; (c) face pressure versus excavation speed; (d) grouting pressure versus excavation speed.

Table 6: Standard values and ranges of excavation speed and TBMPs.

Factors	v (mm/min)	F (kN)	P_N (kPa)	M_T (kN·m)	P_G (kPa)
Parameter range	[20, 44]	[8300, 13100]	[117, 143]	[1294, 2974]	[197, 302]
Standard value	32	9700	132.6	2270	302
Deviation range (%)	[−37.5, 37.5]	[−14.43, 35.05]	[−11.76, 7.84]	[−43.0, 31.01]	[−34.77, 0]

best, whereas the cutter head torque had a deviation interval of 74.01% and was controlled the worst.

(4) Statistical Relationship between TBM Parameters and Excavation Speed. The monitoring results in Figure 6 demonstrated that in the "normal excavation phase" of the XWS, the total thrust and the face pressure were positively correlated with the excavation speed. In particular, the total thrust had a stronger correlation to the excavation speed than the face pressure. In contrast, the cutter head

torque and the primary grouting pressure were negatively correlated with the excavation speed.

3.2. Bow-Tie-Bayesian Network Analysis. The bow-tie analysis combines FT and ET analyses. The FT analysis in bow-tie calculates the occurrence probability of the loss event (LE) as well as the top event (TE). The occurrence probability of the TE can also be obtained from the occurrence probability of the basic event (BE). The events could be evaluated by their logical relationship and their occurrence probability in the BN. Mapping the bow-tie analysis to BN involves converting both FT and ET analyses. Figure 7(a) provides a brief description of calculation steps.

Three importance measures, described in the following Borst and Schoonakker [30], were introduced in the new methodology according to the Bayes theorem. Figure 7(b) gives a brief description of their calculation. In the proposed methodology, the critical nodes that could more easily trigger accidents were obtained by calculating these importance measures.

3.3. Confirming Failure Occurrence Probability. The BT-BN analysis requires knowing the occurrence probability of each basic event (BE). The basic events fall into four categories: environmental failure, operational error, multiple failures, and facility failures. The occurrence rate of facility failures was obtained from the construction log of the XWS for the tunneling project that spanned 179 days (715 segments in total) and was converted into occurrence probability via the following equation:

$$F = 1 - e^{-\lambda t}, \tag{8}$$

where F denotes the occurrence probability of the failure and λ denotes the occurrence rate of the failure.

The occurrence probability of environmental failure, operational error, and multiple failures cannot be readily derived from existing data and was thus estimated via expert opinion. The fuzzy method combines the opinions of different experts in a weighted manner to calculate the fuzzy fault rate (FFR) from the triangular fuzzy numbers or trapezoidal fuzzy numbers proposed by the experts. The occurrence probability of environmental failure, operational error, and multiple failures was then determined from the FFR [34]. The general procedure of the fuzzy method is as follows:

(1) Determine the weight of the opinion of each expert based on the age, education background, work experience, and position of the consulted expert (Table 7). The crude weight score of each expert is calculated via the following equation:

$$S_n = S_{n_a} + S_{n_b} + S_{n_c} + S_{n_d}, \tag{9}$$

where S_n represents the total weight score of the expert. The relative weight score of each expert is calculated via the following equation:

$$W_n = \frac{S_n}{\sum_{n=1}^{m} S_n}, \tag{10}$$

where m represents the number of experts.

(2) The occurrence probability is divided into the following categories: nonoccurrence, absolute low, very low, low, fairly low, medium, fairly high, high, very high, absolute high, or occurrence. The rank value of the categories escalates from 0 for nonoccurrence to 1 for the occurrence (Table 8). The occurrence probability of the event is then evaluated based on the corresponding triangular number or trapezoidal number given by the experts.

(3) Aggregation of the fuzzy numbers. When the fuzzy numbers are all triangular number or trapezoidal number, the aggregated fuzzy numbers of an event is calculated via equation (11) [35]. The aggregated fuzzy number considering the expert weight is shown in equation (12).

$$\widetilde{A}_{\text{aggregated}} = \sum_{n=1}^{m} W_n \otimes \widetilde{A}_n, \tag{11}$$

where $\widetilde{A}_{\text{aggregated}}$ represents the aggregated fuzzified number given by expert m and W_n represents the weight of the expert's opinion:

$$\widetilde{A}_W = \Big(W_1 a_{11} + W_2 a_{21}, W_1 a_{12} + W_2 a_{22}, W_1 a_{12} + W_2 a_{23}, W_1 a_{13} + W_2 a_{24}\Big). \tag{12}$$

(4) After the aggregated fuzzy numbers are determined, the centroid index method (equation (13)) is used to handle the fuzzy numbers and obtain the fuzzy probability score (FPS) [36]:

$$X = \frac{\int g(x)x\,dx}{\int g(x)dx}, \tag{13}$$

where X is the defuzzified output, $g(x)$ is the membership function, and x is the output variable. Assume $\widetilde{A}_n = (a_{n1}, a_{n2}, a_{n3})$ a triangular number and $\widetilde{A}_n = (a_{n1}, a_{n2}, a_{n3})$ a trapezoidal number. The FPS is calculated via equation (14) when a fuzzy number is a triangular number and via equation (15) when the fuzzy number is a trapezoidal number:

$$\text{FPS} = \frac{1}{3}\left(a_{n1} + a_{n2} + a_{n3}\right), \tag{14}$$

$$\text{FPS} = \frac{1}{3}\,\frac{\left(a_{n3} + a_{n4}\right)^2 - a_{n3}a_{n4} - \left(a_{n1} + a_{n2}\right)^2 + a_{n1}a_{n2}}{\left(a_{n3} + a_{n4} - a_{n1} - a_{n2}\right)}. \tag{15}$$

(1) If the logical relationship is AND between events, the TE occurs when all events occur. The probability of TE can be calculated from the following equation

$$F_{\mathrm{TE}} = \prod_{i=1}^{n} F_{\mathrm{BE}_i}. \quad \text{(A)}$$

(2) If the logical relationship is OR between events, the TE occurs when any of the event occurs. The probability of TE can be calculated from the following equation

$$F_{\mathrm{TE}} = 1 - \prod_{i=1}^{n} (1 - F_{\mathrm{BE}_i}). \quad \text{(B)}$$

(3) By definition, in the FT analysis, the probability of TE is the same as that of LE. Similarly, the probability of the initial event (IE) in the ET analysis is the same as that of LE. The probability of OE in ET analysis can be calculated from the following equation

$$F_{\mathrm{OE}_n} = F_{\mathrm{IE}} \cdot \prod_{i=1}^{n} P(E_i = 0) \cdot \prod_{j=1}^{n} P(E_j = 1). \quad \text{(C)}$$

(4) The BN, an inference method based on the Bayes theorem, combines both graph theory and probability theory:

$$P(B \mid A) = \frac{P(A \mid B) \cdot P(B)}{P(A)}. \quad \text{(D)}$$

(a)

(1) The Birnbaum measure (BM), which determines the increment of the occurrence probability of TE when BE occurs, is shown in the following equation

$$I_{\mathrm{BE}}^{\mathrm{BM}} = P(\mathrm{TE} \mid \mathrm{BE} = 1) - P(\mathrm{TE} \mid \mathrm{BE} = 0). \quad \text{(E)}$$

where $P(\mathrm{TE} \mid \mathrm{BE} = 1)$ denotes the occurrence probability of TE when BE occurs and $P(\mathrm{TE} \mid \mathrm{BE} = 0)$ denotes the occurrence probability of TE when BE does not occur.

(2) Risk achievement worth (RAW) evaluates the impact of BE on TE when the probability of BE is considered. The RAW is adjusted by the probability of TE and BE as shown in the following equation

$$I_{\mathrm{BE}}^{\mathrm{RAW}} = I_{\mathrm{BE}}^{\mathrm{BM}} \cdot \frac{P(\mathrm{BE})}{P(\mathrm{TE})}. \quad \text{(F)}$$

where $P(\mathrm{BE})$ denotes the occurrence probability of BE and $P(\mathrm{TE})$ denotes the occurrence probability of TE under all circumstances.

(3) The Fussell–Vesely (FV) importance, which describes the contribution of BE to system fault, is shown in the following equation:

$$I_{\mathrm{BE}}^{\mathrm{FV}} = \frac{P(\mathrm{TE}) - P(\mathrm{TE} \mid \mathrm{BE} = 0)}{P(\mathrm{TE})}. \quad \text{(G)}$$

(b)

Figure 7: Bow-tie-Bayesian network analysis. Calculation of (a) event probability and (b) importance measures.

Table 7: Weight scores for experts.

Factor	Category	Score
Age (a)	<30	1
	30–39	2
	40–49	3
	≥50	4
Education (b)	High school	1
	College	2
	Bachelor	3
	Master	4
	Ph.D.	5
Work experience (c)	<5 years	1
	5–10 years	2
	11–20 years	3
	21–30 years	4
	≥30 years	5
Position (d)	Worker	1
	Technician	2
	Junior scholar/engineer	3
	Senior scholar/engineer	4

(5) Finally, the FPS is converted to FFR via equation (16) [37], and the FFR is further converted to the occurrence probability of environmental failure, operational error, and multiple failures (equation (8)):

Table 8: Rank value of each category.

Classified occurrence probability	Rank value
Nonoccurrence	0
Absolute low	0.1
Very low	0.2
Low	0.3
Fairly low	0.4
Medium	0.5
Fairly high	0.6
High	0.7
Very high	0.8
Absolute high	0.9
Occurrence	1.0

$$\mathrm{FFR} = \begin{cases} \dfrac{1}{10^k}, & \mathrm{FPS} \neq 0, \\ 0, & \mathrm{FPS} = 0, \\ k = 2.301 \times \left[\dfrac{(1 - \mathrm{FPS})}{\mathrm{FPS}}\right]^{1/3}. \end{cases} \quad (16)$$

4. Results

4.1. Analysis of Excessive Surface Settlement in Normal Tunnel Excavation. Figure 8 shows that the normal excavation

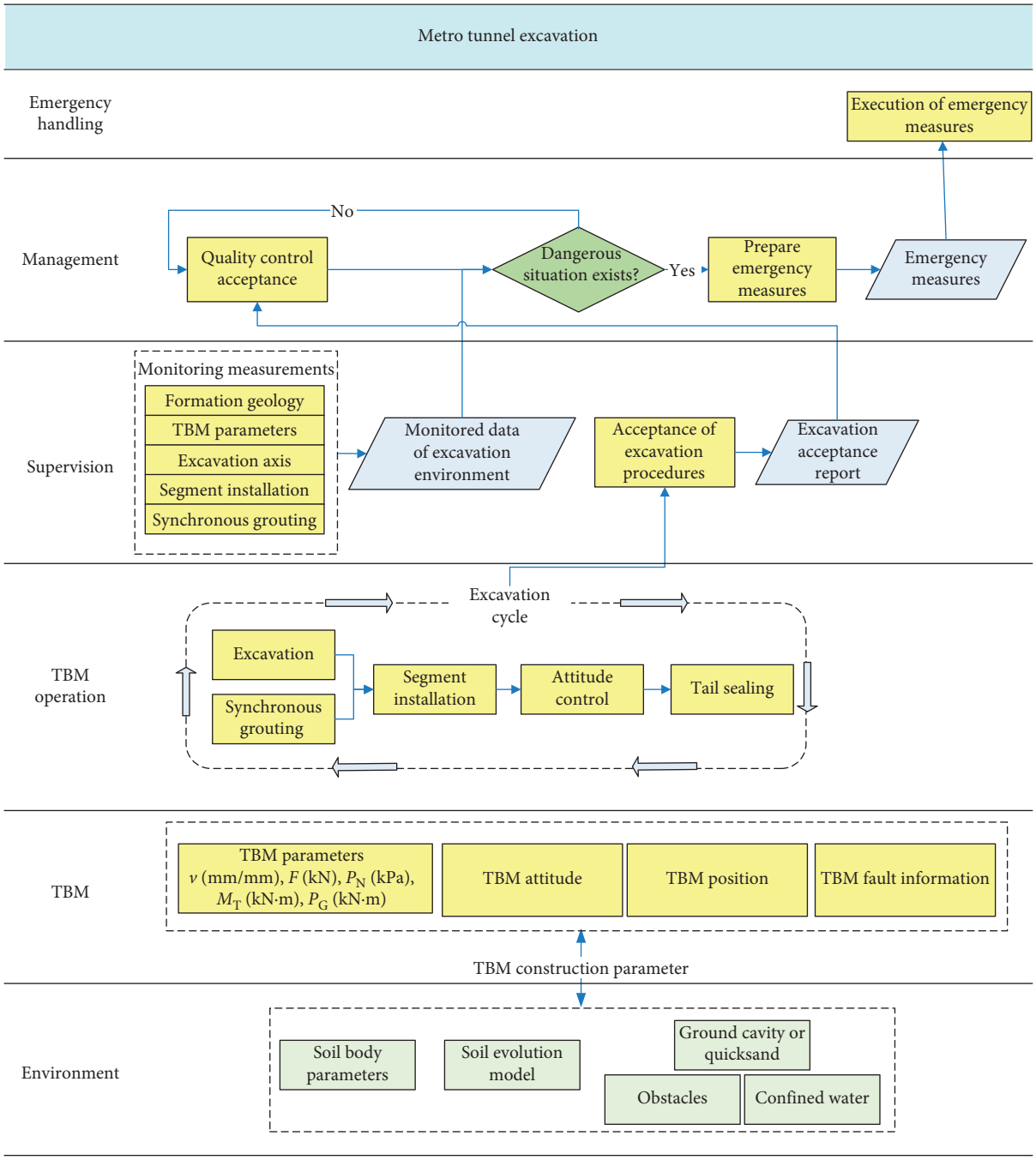

Figure 8: System diagram of the "normal excavation phase."

phase involves the environment, TBM operation, supervision, management, and emergency handling. Risk analysis of the "normal excavation phase" in soft soil engineering based on the XWS allows the identification of potential risk factors that may trigger surface settlement and consequently lead to accidents. Eskesen et al. have described three principles for risk analysis as follows: (1) eliminate risk factors that are easy to detect and can be controlled timely and effectively, (2) eliminate risk factors with low occurrence probability and no catastrophic consequences, and (3) combine risk factors with similar loss consequences [38]. Accordingly, the risk factors during shield tunneling were organized into three basic categories: improper control of excavation parameters (e.g., poor control of face pressure), catastrophic geology (e.g., ground cavity or flow sand), and unforeseeable factors (e.g., segment damage). Figure 9 shows the bow-tie model built from the categorized factors for the risk of surface collapse caused by excessive surface settlement during shield tunneling. OEs of various degrees were successfully predicted based on the CEs (Figure 9). Many risk factors exist in any given surface collapse. In this section, based on the previous calculation results in Section 3.1, we selected the manageable shield excavation parameters (shield total thrust, grouting pressure, cutter head torque, soil pressure, etc.) in the "normal

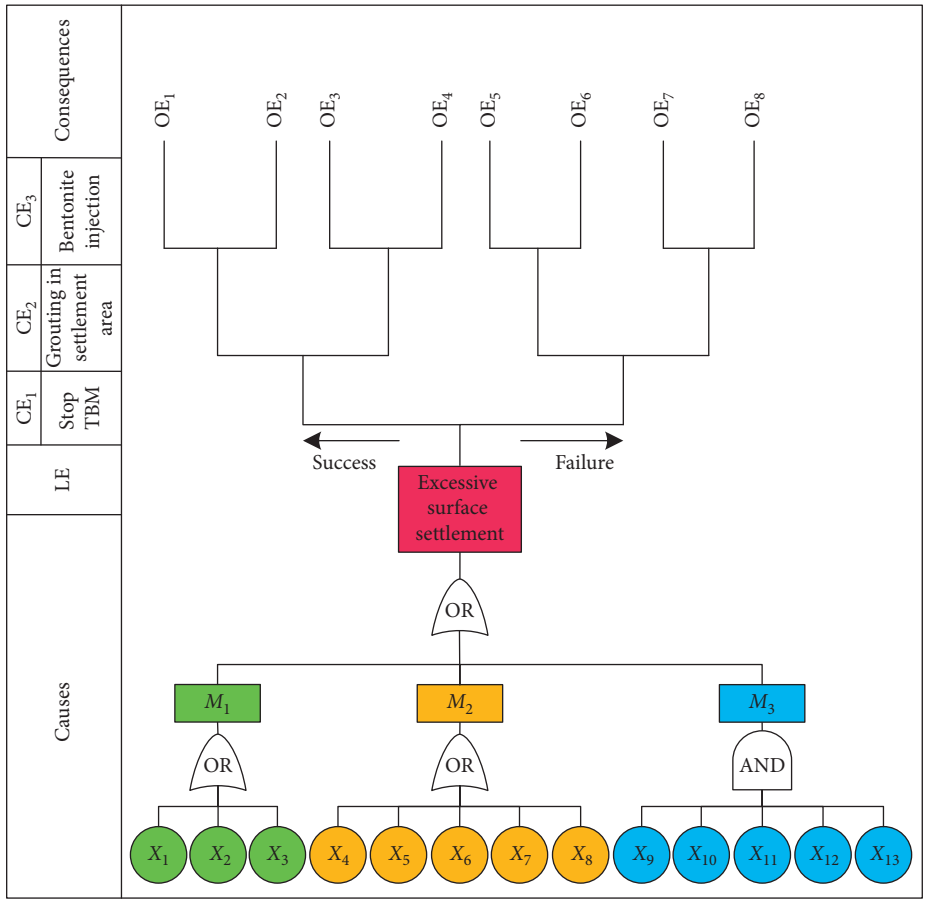

Figure 9: Diagram of bow-tie analysis for excessive surface settlement.

excavation phase" as the base events, assigning their weights according to Section 3.3, and then performed PSA analysis.

As mentioned earlier, the "normal excavation phase" is under the influence of excavation parameters, catastrophic geology, and unforeseeable factors. Surface settlement can occur once the condition deteriorates. Here we set excessive surface settlement as the TE in the FT analysis. Meanwhile, the tunneling system has a built-in emergency management system. Upon excessive surface settlement, the emergency management system will start to shut down the TBM timely. Hence, in the ET analysis, the excessive surface settlement is set as the IE and TBM shutdown is set as the CE. OEs of various degrees are obtained based on the considered CE. Finally, the surface settlement is set as the LE to connect the FT and the ET and furnish the BT model (Figure 9; Table 9). Eight OEs of various degrees were predicted based on the CEs, including surface collapse events OE_3, OE_4, OE_6, OE_7, and OE_8 (Figure 9; Table 10). The TBM shuts down if CE_1 occurs and continues to operate if otherwise.

The BN-BT model for excessive surface settlement is constructed by mapping the FT and ET analyses in the BT (Figure 9) model to BN (Figure 10). All the nodes of BN have previously been described in the BT except the node OE, which is the consequence node. OE is added to accommodate the outcomes of BT. By connecting the node of excessive surface settlement to OE, another state also called the safe state is added to the state set. It includes consequences OE_1 to OE_8 to account for the nonoccurrence of the top event, i.e., when excessive surface settlement = controlled. To show the dependence among the safety barriers and the top event, causal arcs are also drawn between TBM shutdown and grouting in the settlement area and bentonite injection to soil chamber and TBM shield. It is worth noting that since various combinations of the failure and success of the sequential safety barriers result in different consequences in the BT, all the safety nodes of BN are connected to node OE.

4.2. Determination of Event Occurrence Probability. The maximum surface settlement that resulted from the aberration of the ith TBM parameter is denoted as $\delta_{\max,i}$. The probability of safety accident becomes higher when $\delta_{\max,i}$ approaches the permitted surface settlement δ_i. When $\delta_{\max,i} = \delta_i$, the accident will occur as soon as the TBM parameter gives rise to a surface settlement of $\delta_{\max,i}$. The probability of equipment fault for the normal excavation system was calculated via equation (8) from the engineering log data of the XWS over 179 days of construction (715 segments rings in total). The construction of all 715 rings fell within the "normal excavation phase" as was defined by the fuzzy statistical test ($v = 20$–44 mm/min). Table 11 lists the calculation results.

Table 9: Details of bow-tie components in Figure 9.

Event	Symbol	Logic link type	Failure model
Ground settlement	Excessive surface settlement	OR gate	—
Catastrophic geology	M_1	OR gate	—
Unforeseeable factors	M_2	OR gate	—
Excavation parameters	M_3	AND gate	—
Confined water	X_1	—	Environmental failure
Ground cavity or flow sand	X_2	—	Environmental failure
Obstacles	X_3	—	Environmental failure
Segment damage	X_4	—	Operational error
Abnormal TBM shutdown	X_5	—	Multiple failure
Seal failure at shield tail	X_6	—	Multiple failure
Excessive deviation from axis	X_7	—	Operational error
Equipment failure	X_8	—	Multiple failure
Untimely grouting	X_9	—	Facility failure
Excessive cutter head torque	X_{10}	—	Facility failure
Improper control of face pressure	X_{11}	—	Facility failure
Excessive thrust	X_{12}	—	Facility failure
Improper control of excavation speed	X_{13}	—	Facility failure
TBM shutdown	CE_1	—	Multiple failure
Grouting in settlement area	CE_2	—	Multiple failure
Bentonite injection to soil chamber and TBM shield	CE_3	—	Multiple failure

Table 10: Analysis of event occurrence.

Symbol	Event
OE_1	Excessive surface settlement
OE_2	Grouted cutter head and shield, excessive surface settlement, and minor property damage
OE_3	Minor surface collapse and property damage
OE_4	Moderate surface collapse, major property damage, and minor casualties
OE_5	Excessive surface settlement
OE_6	Grouted cutter head and shield, moderate surface collapse, and minor property damage
OE_7	Moderate surface collapse and major property damage
OE_8	Severe surface collapse, major property damage, and major casualties

To address the uncertainty regarding the events of environmental failure, operational error, and multiple failure, six domain experts who participated in the construction of the Wuhan metro system, including two senior engineers, one senior academic professor, one technical consultant, one junior engineer, and one worker, were invited to evaluate the occurrence probability of events that cannot be readily derived from existing data (Table 12). The weights of their opinion were then calculated by using equations (9) and (10), and the distribution of each opinion weight is shown in Figure 11.

In addition, Table 13 lists the expert opinions regarding the events of environmental failure, operational error, and multiple failures in the form of fuzzy numbers based on Table 8. The fuzzy numbers were aggregated via equations (12) and converted to FPS and FFR via equations (13)–(16) (Table 14). The occurrence probabilities were finally derived from FFR (Table 14). Generally, the expert knowledge is considered as a scarce resource which cannot provide universal consultation or real-time guidance. Thus, there is much room to improve the data use efficiency.

4.3. Update in Occurrence Probability of LE and OE. The occurrence probability of basic events is calculated as described in Section 4.2, including the occurrence probability of facility failure from the engineering log data of the XWS as well as that of environmental failure, operational error, and multiple failures derived from expert opinion. The occurrence probability of excessive surface settlement (LE) is determined via equations (A) and (B) by considering the logical relationship between events in Figure 7. Finally, the occurrence probability of OEs including surface collapse can be calculated via equation (C) in the figure by mapping the FT and ET analyses in the BT model to BN. Figure 12 shows the occurrence probabilities of the LE (i.e., excessive surface settlement) and that of the OEs.

The above analysis shows that the occurrence probability of excessive surface settlement within one year is 0.8299 (Figure 12). This occurrence probability of surface collapse (OE_3, OE_4, OE_6, OE_7, and OE_8) may be decreased when emergency measures are put in place, including grouting in settlement area and bentonite injection to soil chamber and TBM shield. However, these measures cannot help to reduce minor accidents since the occurrence probability remains at high levels for OE_1, OE_2, and OE_5. Admittedly, grouting and bentonite injection are necessary measures and they can decrease the effects of excessive surface settlement during shield tunneling. However, the key point of avoiding outcome events including surface collapse to ensure project safety is to prevent the excessive surface settlement from occurring in the first place. Hence, we sought to determine the key nodes leading to excessive surface settlement via BT-BN analysis and propose the corresponding preventive measures.

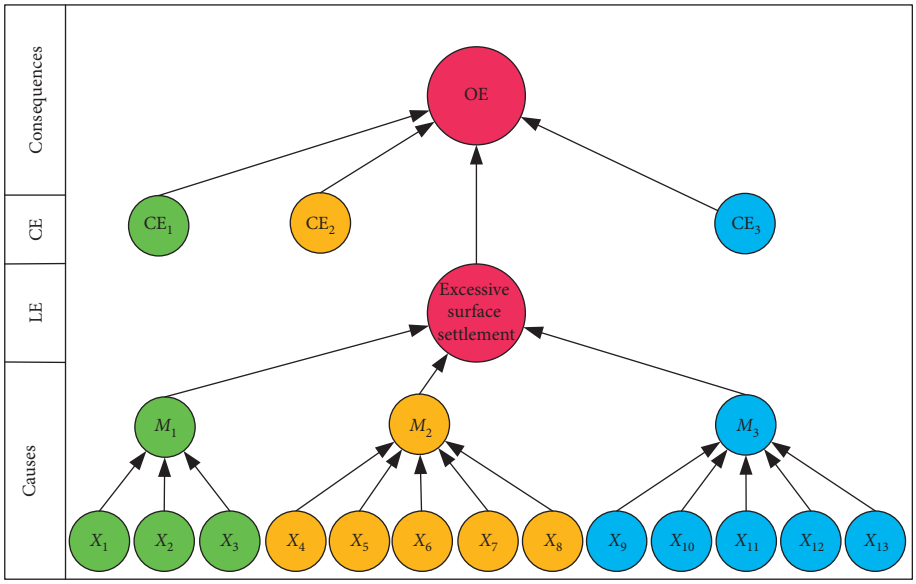

Figure 10: Bow-tie chart of excessive surface settlement.

Table 11: Probability of equipment fault.

Event	Surface settlement $\delta_{\max,i}$ (mm)	Permitted surface settlement δ_i (mm)	Value of TBM parameter	Occurrence rate (d^{-1})	Occurrence probability (in 1 year)
X_9	8.9	15	302 kPa	$1.0675e-04$	$3.82e-02$
X_{10}	8.4	10	2974 kN·M	$1.7792e-04$	$6.29e-02$
X_{11}	8.6	15	143 kPa	$7.1167e-05$	$2.56e-02$
X_{12}	9.8	15	13100 kN	$1.4233e-04$	$5.06e-02$
X_{13}	12.0	15	41 mm/min	$2.8467e-04$	$9.87e-02$

All data were obtained from the operation log of the XWS.

Table 12: Characteristics of experts participated in the occurrence probability evaluation.

Expert	Age	Education	Service (years)	Professional position
1	56	High school	25	Worker
2	35	Master	10	Technician
3	41	Master	15	Junior engineer
4	47	Bachelor	20	Senior engineer
5	50	PhD	18	Senior academic
6	59	PhD	30	Senior engineer

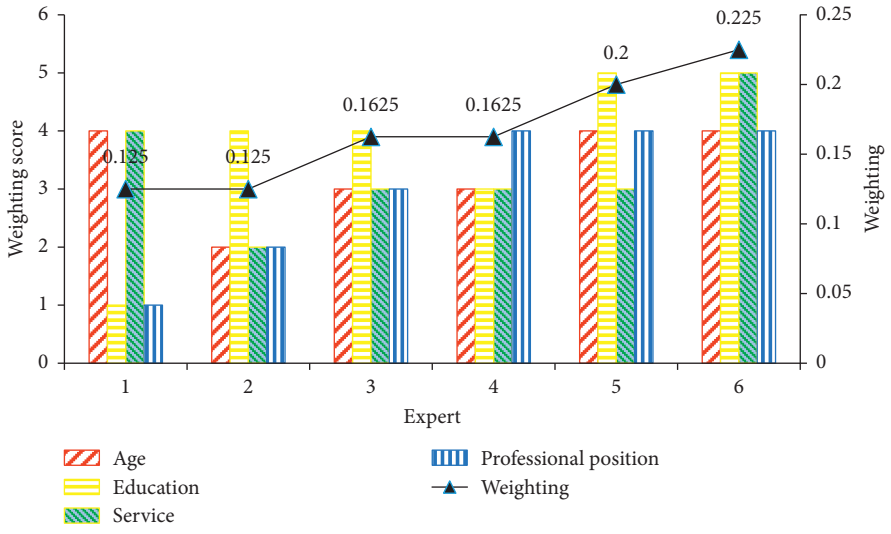

Figure 11: Distribution of each expert opinion weight.

Table 13: Expert opinion on environmental failure, operational error, and multiple failures.

Event	Fuzzy numbers proposed by each expert		
X_1	Expert 1 (0.2, 0.3, 0.4, 0.5)	Expert 2 (0.1, 0.2, 0.3, 0.5)	Expert 3 (0.2, 0.3, 0.4, 0.5)
	Expert 4 (0.1, 0.2, 0.3, 0.4)	Expert 5 (0.1, 0.2, 0.3, 0.5)	Expert 6 (0.1, 0.2, 0.3, 0.5)
X_2	Expert 1 (0.1, 0.2, 0.3, 0.5)	Expert 2 (0.2, 0.3, 0.4)	Expert 3 (0.1, 0.2, 0.4, 0.5)
	Expert 4 (0.1, 0.2, 0.3, 0.4)	Expert 5 (0.2, 0.3, 0.5)	Expert 6 (0.1, 0.2, 0.3, 0.5)
X_3	Expert 1 (0.1, 0.2, 0.4, 0.5)	Expert 2 (0.1, 0.2, 0.3, 0.5)	Expert 3 (0.1, 0.3, 0.4)
	Expert 4 (0.1, 0.2, 0.3, 0.4)	Expert 5 (0.1, 0.2, 0.3)	Expert 6 (0.1, 0.2, 0.3)
X_4	Expert 1 (0.2, 0.3, 0.4, 0.5)	Expert 2 (0.1, 0.2, 0.3, 0.5)	Expert 3 (0.2, 0.3, 0.4, 0.5)
	Expert 4 (0.2, 0.3, 0.4)	Expert 5 (0.2, 0.3, 0.5)	Expert 6 (0.1, 0.2, 0.3, 0.5)
X_5	Expert 1 (0.1, 0.3, 0.4)	Expert 2 (0.1, 0.2, 0.3, 0.5)	Expert 3 (0.2, 0.3, 0.5)
	Expert 4 (0.1, 0.2, 0.3, 0.4)	Expert 5 (0.2, 0.3, 0.5)	Expert 6 (0.1, 0.2, 0.3)
X_6	Expert 1 (0.2, 0.3, 0.4)	Expert 2 (0.1, 0.2, 0.3, 0.5)	Expert 3 (0.2, 0.3, 0.5)
	Expert 4 (0.1, 0.2, 0.3, 0.4)	Expert 5 (0.2, 0.3, 0.5)	Expert 6 (0.1, 0.2, 0.4, 0.5)
X_7	Expert 1 (0.1, 0.2, 0.4, 0.5)	Expert 2 (0.1, 0.2, 0.3, 0.5)	Expert 3 (0.2, 0.3, 0.4)
	Expert 4 (0.1, 0.2, 0.3, 0.4)	Expert 5 (0.1, 0.2, 0.3, 0.5)	Expert 6 (0.1, 0.3, 0.5)
X_8	Expert 1 (0.1, 0.3, 0.4, 0.5)	Expert 2 (0.1, 0.2, 0.3, 0.4)	Expert 3 (0.2, 0.3, 0.4)
	Expert 4 (0.2, 0.3, 0.4)	Expert 5 (0.1, 0.2, 0.3, 0.5)	Expert 6 (0.1, 0.2, 0.3)
CE_1	Expert 1 (0.2, 0.3, 0.4, 0.5)	Expert 2 (0.2, 0.3, 0.5)	Expert 3 (0.2, 0.3, 0.4, 0.5)
	Expert 4 (0.1, 0.2, 0.3, 0.4)	Expert 5 (0.1, 0.2, 0.3, 0.5)	Expert 6 (0.1, 0.2, 0.4, 0.5)
CE_2	Expert 1 (0.2, 0.3, 0.4)	Expert 2 (0.1, 0.2, 0.5)	Expert 3 (0.2, 0.3, 0.4, 0.5)
	Expert 4 (0.1, 0.2, 0.3, 0.4)	Expert 5 (0.1, 0.2, 0.3, 0.5)	Expert 6 (0.1, 0.3, 0.5)
CE_3	Expert 1 (0.2, 0.3, 0.4)	Expert 2 (0.1, 0.2, 0.3, 0.5)	Expert 3 (0.3, 0.4, 0.5)
	Expert 4 (0.1, 0.2, 0.3, 0.4)	Expert 5 (0.1, 0.2, 0.4, 0.5)	Expert 6 (0.1, 0.2, 0.3, 0.5)

4.4. Identify Key Nodes and Provide Safety Measures. In order to find the key nodes leading to excessive surface settlement, the importance measure of each event was calculated via equations (E)–(G) in Figure 7, as shown in Table 15. Assume the number of events as "n." The normalized weight R^* could be calculated from the importance measure I_i via the following equation:

$$R^* = \frac{I_i}{\sum_{i=1}^{n} I_i} \times 100. \tag{17}$$

After the normalized weight R^* is calculated for each importance measure, the total weight $R_{\#}^*$ could be calculated via equation (18). The total weight $R_{\#}^*$ of events was finally ranked in descending order to find the key nodes, as shown in Table 16:

$$R_{\#}^* = R_{\mathrm{BM}}^* + R_{\mathrm{RAW}}^* + R_{\mathrm{FV}}^*. \tag{18}$$

It can be seen that X_6 (seal failure at shield tail), X_1 (confined water), X_2 (ground cavity or flow sand), X_5 (abnormal TBM shutdown), and X_7 (excessive deviation from axis) have far higher weight than other events and are thus the key nodes to accidents related to excessive surface settlement. Measures can be taken to particularly ensure safety at these nodes. The occurrence probability of excessive surface settlement can be reduced by 66% when X_6, X_1, X_2, X_5, and X_7 are ensured safe (Figure 13).

Table 14: Calculation of FPS, FFR, and the occurrence probability of environmental failure, operational error, and multiple failures.

Event	Aggregated fuzzy numbers	FPS	FFR (d^{-1})	Failure probability (in 1 year)
X_1	(0.1288, 0.2288, 0.3288, 0.4838)	0.2951	$8.3969e-04$	$2.6402e-1$
X_2	(0.1325, 0.2325, 0.3163, 0.4713)	0.2909	$8.0032e-04$	$2.5336e-1$
X_3	(0.1000, 0.2163, 0.2700, 0.3825)	0.2420	$4.2986e-04$	$1.4518e-1$
X_4	(0.0450, 0.0900, 0.1125, 0.1800)	0.1082	$2.2492e-05$	$8.1803e-3$
X_5	(0.1363, 0.2488, 0.2775, 0.4263)	0.2747	$6.6022e-04$	$2.14155e-1$
X_6	(0.1488, 0.2488, 0.3225, 0.4713)	0.3004	$8.9125e-04$	$2.7770e-1$
X_7	(0.1163, 0.2388, 0.3125, 0.4675)	0.2855	$7.5157e-04$	$2.4002e-1$
X_8	(0.1450, 0.2538, 0.2950, 0.3100)	0.2463	$4.5643e-04$	$1.5338e-1$
CE_1	(0.1413, 0.2413, 0.3513, 0.4838)	0.3058	$9.4598e-04$	$2.9202e-1$
CE_2	(0.1288, 0.2513, 0.3038, 0.4713)	0.2916	$8.0679e-04$	$2.5496e-1$
CE_3	(0.1450, 0.2450, 0.3363, 0.4713)	0.3010	$8.9722e-04$	$2.7937e-1$

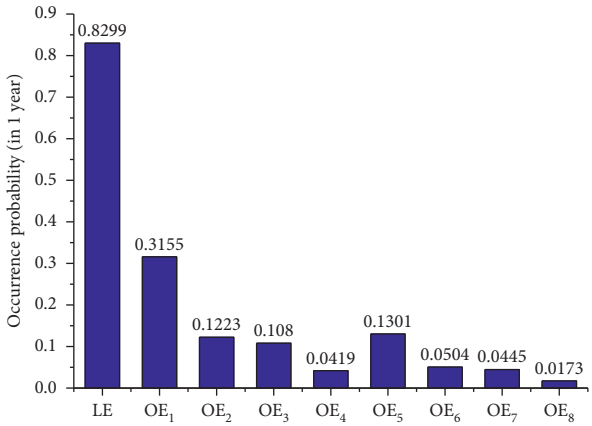

Figure 12: Occurrence probability of surface settlement and other outcome events.

Table 15: Calculation of importance measure of influential factors.

Symbol	Importance measure		
	BM	RAW	FV
X_1	$2.311e-1$	$7.352e-02$	$7.352e-02$
X_2	$2.279e-1$	$6.958e-02$	$6.958e-02$
X_3	$1.990e-1$	$3.481e-02$	$3.481e-02$
X_4	$1.716e-1$	$1.691e-03$	$1.691e-03$
X_5	$2.165e-1$	$5.587e-02$	$5.587e-02$
X_6	$2.356e-1$	$7.884e-02$	$7.884e-02$
X_7	$2.239e-1$	$6.476e-02$	$6.476e-02$
X_8	$2.010e-1$	$3.715e-02$	$3.715e-02$
X_9	$1.370e-6$	$6.306e-08$	$6.306e-08$
X_{10}	$8.300e-7$	$6.291e-08$	$6.291e-08$
X_{11}	$2.040e-6$	$6.293e-08$	$6.293e-08$
X_{12}	$1.030e-6$	$6.280e-08$	$6.280e-08$
X_{13}	$5.300e-7$	$6.303e-08$	$6.303e-08$

In accordance with the predictive and diagnostic analysis results using the established model, some safety measures for key nodes are displayed in time to reduce the excessive surface settlement risk during the tunnel excavation.

(1) The nodes X_5 (abnormal TBM shutdown) and X_7 (excessive deviation from the axis) mostly involve operational error. Safety management and supervision need to be strengthened at the construction site to eliminate such errors and ensure that the TBM is operated properly. Besides, an advanced real-time laser locator may help to alarm in the case of large axial deviation.

(2) The nodes X_1 (confined water) and X_2 (ground cavity or flow sand) belong to environmental failure. In order to reduce the influence of environmental failure, careful geological exploration should be carried out before tunneling to identify the poor geological and

Table 16: Ranking results of the key events.

Rank	Symbol	Normalization weighting ($R^*_{\#}$)			Total weighting ($R^*_{\#}$)
		R^*_{BM}	R^*_{RAW}	R^*_{FV}	
1	X_6	13.805	18.942	18.942	51.689
2	X_1	13.541	17.664	17.664	48.869
3	X_2	13.354	16.717	16.717	46.788
4	X_7	13.120	15.559	15.559	44.238
5	X_5	12.686	13.423	13.423	39.532
6	X_8	11.778	8.926	8.9255	29.629
7	X_3	11.661	8.363	8.363	28.387
8	X_4	10.055	0.406	0.406	10.868
9	X_{11}	0.0002	$1.512e-05$	$1.512e-05$	$1.498e-04$
10	X_9	$8.028e-05$	$1.515e-05$	$1.515e-05$	$1.106e-04$
11	X_{12}	$6.035e-05$	$1.509e-05$	$1.509e-05$	$9.053e-05$
12	X_{10}	$4.863e-05$	$1.511e-05$	$1.511e-05$	$7.886e-05$
13	X_{13}	$3.106e-05$	$1.514e-05$	$1.514e-05$	$6.134e-05$
Total		100	100	100	100

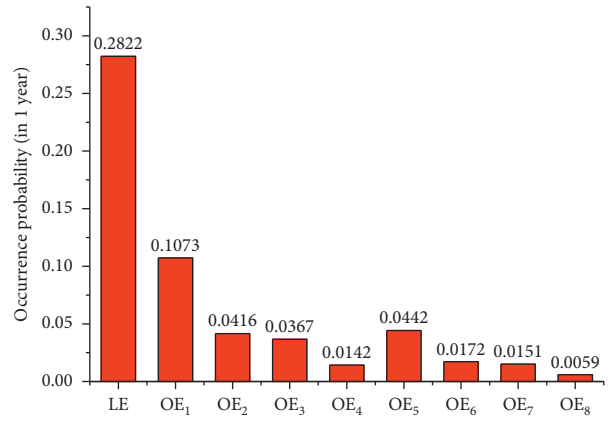

Figure 13: Occurrence probability when safety is ensured at key nodes.

hydrological conditions that may be encountered. During excavation, the advanced geological prediction technology may be employed to detect adverse geological and hydrological conditions ahead of the TBM in real time, including confined water, ground cavity, and flow sand.

(3) Node X_6 (seal failure at shield tail) belongs to multiple failures. The quality of the tail brush needs to be enhanced, and tail brush should promptly be replaced when it is worn.

By adopting corresponding safety measures in shield tunnel excavation, the occurrence probability of various degrees of surface collapse (OE_3, OE_4, OE_6, OE_7, and OE_8) was significantly decreased (Figure 13). Finally, the TBMs successfully passed through the left track of DCS on March 3, 2017, and the right track on June 11, 2017, without any surface collapse accident, demonstrating the effectiveness of our proposed hybrid method.

5. Conclusions and Future Works

In this work, we first defined the "normal excavation phase" of shield tunneling based on the fuzzy statistical test theory. Data were extracted from the construction log of the XWS in the Wuhan metro line 7 to determine the occurrence probability of facility fault, and expert opinions were solicited to determine the occurrence probability of environmental failure, operational error, and multiple failures. Probabilistic safety assessment (PSA) of the normal shield tunnel excavation system was then performed accordingly.

We employed the bow-tie analysis to evaluate the occurrence of excessive surface settlement during normal tunnel excavation. The presence of emergency measures could reduce the occurrence probability of surface collapse caused by excessive surface settlement (OE_3, OE_4, OE_6, OE_7, and OE_8) but have limited effect on the prevention of accidents of OE_1, OE_2, and OE_5. It is essential to decrease the probability of excessive surface settlement in order to prevent the resulting outcome events (OEs).

By mapping the bow-tie analysis to Bayesian networks (i.e., BT-BN analysis), we determined the key nodes that could cause excessive surface settlement (LE). The key nodes included the following: X_6 (seal failure at shield tail), X_1 (confined water), X_2 (ground cavity or flow sand), X_5 (abnormal TBM shutdown), and X_7 (excessive deviation from the axis). Effective safety measures at these nodes could reduce the occurrence probability of excessive surface settlement (LE) by 66%.

To ensure safety, careful geological exploration should be carried out before the tunneling project. During the tunneling, safety management and supervision should be strengthened at the construction site. Advanced geological prediction technology should be used to detect poor geological and hydrological conditions ahead of the TBM in real time. Advanced laser locator should be used to monitor and alarm excessive axial deviation. The quality of the tail brush should be improved, and tail brush should be replaced timely when it becomes worn. The occurrence probability of excessive surface settlement was decreased by adopting these safety measures, and the occurrence of the resulting surface collapse was subsequently decreased.

Data Availability

The data used to support the findings of this study are available from the corresponding author upon request.

Conflicts of Interest

The authors declare that there are no conflicts of interest regarding the publication of this paper.

Acknowledgments

The authors thank the workers, foremen, and safety coordinators of the main contractors for their participation. The authors also wish to thank the engineers Yun Zhang and Peilun Tu for assistance in gathering field data.

References

[1] T. Zhao, W. Liu, and Z. Ye, "Effects of water inrush from tunnel excavation face on the deformation and mechanical performance of shield tunnel segment joints," *Advances in Civil Engineering*, vol. 2017, Article ID 5913640, 9 pages, 2017.

[2] W. Liu, T. Zhao, W. Zhou, and J. Tang, "Safety risk factors of metro tunnel construction in China: an integrated study with EFA and SEM," *Safety Science*, vol. 105, pp. 98–113, 2018.

[3] K. Li, "Hangzhou metro site collapse accident," 2008, http://news.sohu.com/20081115/n260653551.shtml.

[4] S. Liu, "Construction of Nanchang metro line 2 construction section pavement collapses," 2017, http://news.sohu.com/20160514/n449414512.shtml.

[5] R. B. Peck, "Deep excavations and tunneling in soft ground," *7th International Conference on Soil Mechanics and Foundation Engineering*, vol. 7, no. 3, pp. 225–290, 1969.

[6] P. B. Attewell, I. W. Farmer, and N. H. Glossop, "Ground deformation caused by tunnelling in a silty alluvial clay," *Ground Engineering*, vol. 11, no. 8, pp. 32–41, 1978.

[7] W. J. Rankin, "Ground movements resulting from urban tunnelling: predictions and effects," *Geological Society, London, Engineering Geology Special Publications*, vol. 5, no. 1, pp. 79–92, 1988.

[8] P. B. Attewell and J. P. Woodman, "Predicting the dynamics of ground settlement and its derivatives caused by tunneling in soil," *Ground Engineering*, vol. 15, no. 8, pp. 13–20, 1982.

[9] M. P. O'Reilly and B. M. New, "Settlement above tunnels in the United Kingdom—their magnitude and prediction: in tunnelling 82, proceedings of the 3rd international symposium, brighton, 7–11 June 1982, P173–181. Publ London: IMM, 1982," *International Journal of Rock Mechanics & Mining Sciences & Geomechanics Abstracts*, vol. 20, no. 1, pp. 1–18, 1983.

[10] R. J. Mair, R. N. Taylor, and A. Bracegirdle, "Subsurface settlement profiles above tunnels in clays," *Géotechnique*, vol. 45, no. 2, pp. 361-362, 1995.

[11] X. L. Yang and J. M. Wang, "Ground movement prediction for tunnels using simplified procedure," *Tunnelling and Underground Space Technology*, vol. 26, no. 3, pp. 462–471, 2011.

[12] B. Zeng and D. Huang, "Soil deformation induced by Double-O-tube shield tunneling with rolling based on stochastic medium theory," *Tunnelling and Underground Space Technology*, vol. 60, pp. 165–177, 2016.

[13] C. Shi, C. Cao, and M. Lei, "An analysis of the ground deformation caused by shield tunnel construction combining an elastic half-space model and stochastic medium theory," *KSCE Journal of Civil Engineering*, vol. 21, no. 5, pp. 1933–1944, 2017.

[14] T. Hagiwara, R. J. Grant, M. Calvello, and R. N. Taylor, "The effect of overlying strata on the distribution of ground movements induced by tunnelling in clay," *Soils & Foundations*, vol. 39, no. 3, pp. 63–73, 1999.

[15] V. Fargnoli, D. Boldini, and A. Amorosi, "TBM tunnelling-induced settlements in coarse-grained soils: the case of the new Milan underground line 5," *Tunnelling and Underground Space Technology*, vol. 38, no. 3, pp. 336–347, 2013.

[16] V. Fargnoli, C. G. Gragnano, D. Boldini, and A. Amorosi, "3D numerical modelling of soil-structure interaction during EPB tunnelling," *Géotechnique*, vol. 65, no. 1, pp. 23–37, 2015.

[17] GB 50911-2013, *Code for Monitoring Measurement of Urban Rail Transit Engineering*, China Construction Industry Press, Beijing, China, 2014.

[18] S. Suwansawat and H. H. Einstein, "Artificial neural networks for predicting the maximum surface settlement caused by EPB shield tunneling," *Tunnelling and Underground Space Technology*, vol. 21, no. 2, pp. 133–150, 2006.

[19] J. Sun, J. Zhou, X. Gong, and M. Zhang, "Theory of soil environment stability and deformation control under influence of construction disturbance," *Journal of Tongji University*, vol. 32, no. 10, pp. 1261–1269, 2004.

[20] C. Jacinto, C. Silva, P. Swuste, T. Koukoulaki, and A. Targoutzidis, "A semi-quantitative assessment of occupational risks using bow-tie representation," *Safety Science*, vol. 48, no. 8, pp. 973–979, 2010.

[21] P. Cherubin, S. Pellino, and A. Petrone, "Baseline risk assessment tool: a comprehensive risk management tool for process safety," *Process Safety Progress*, vol. 30, no. 3, pp. 251–260, 2011.

[22] A. Targoutzidis, "Incorporating human factors into a simplified "bow-tie" approach for workplace risk assessment," *Safety Science*, vol. 48, no. 2, pp. 145–156, 2010.

[23] A. S. Markowski and A. Kotynia, ""Bow-tie" model in layer of protection analysis," *Process Safety and Environmental Protection*, vol. 89, no. 4, pp. 205–213, 2011.

[24] R. Ferdous, F. Khan, R. Sadiq, P. Amyotte, and B. Veitch, "Analyzing system safety and risks under uncertainty using a bow-tie diagram: an innovative approach," *Process Safety and Environmental Protection*, vol. 91, no. 1-2, pp. 1–18, 2013.

[25] L. Purton, R. Clothier, and K. Kourousis, "Assessment of technical airworthiness in military aviation: implementation and further advancement of the bow-tie model," *Procedia Engineering*, vol. 80, no. 17, pp. 529–544, 2014.

[26] A. Badreddine and N. B. Amor, "A Bayesian approach to construct bow tie diagrams for risk evaluation," *Process Safety & Environmental Protection*, vol. 91, no. 3, pp. 159–171, 2013.

[27] N. Khakzad, F. Khan, and P. Amyotte, "Dynamic risk analysis using bow-tie approach," *Reliability Engineering & System Safety*, vol. 104, pp. 36–44, 2012.

[28] Z. Bilal, K. Mohammed, and H. Brahim, "Bayesian network and bow tie to analyze the risk of fire and explosion of pipelines," *Process Safety Progress*, vol. 36, no. 2, pp. 202–212, 2016.

[29] M. Abimbola, F. Khan, and N. Khakzad, "Risk-based safety analysis of well integrity operations," *Safety Science*, vol. 84, pp. 149–160, 2016.

[30] M. V. D. Borst and H. Schoonakker, "An overview of PSA importance measures," *Reliability Engineering & System Safety*, vol. 72, no. 3, pp. 241–245, 2001.

[31] L. A. Zadeh, "Probability measures of fuzzy events," *Journal of Mathematical Analysis and Applications*, vol. 23, no. 2, pp. 421–427, 1968.

[32] E. Leca, "Settlements induced by tunneling in soft ground," *Tunnelling & Underground Space Technology*, vol. 22, no. 2, pp. 119–149, 2007.

[33] R. J. Mair, "Tunnelling and geotechnics: new horizons," *Géotechnique*, vol. 58, no. 9, pp. 695–736, 2008.

[34] Y. Fang, K. Xu, X. Yao, and Y. Li, "Fuzzy Bayesian network-bow-tie analysis of gas leakage during biomass gasification," *PLoS One*, vol. 11, no. 7, Article ID e0160045, 2016.

[35] H. M. Hsu and C. T. Chen, "Aggregation of fuzzy opinions under group decision making," *Fuzzy Sets & Systems*, vol. 79, no. 3, pp. 279–285, 1996.

[36] S.-J. Chen and S.-M. Chen, "Fuzzy risk analysis based on the ranking of generalized trapezoidal fuzzy numbers," *Applied Intelligence*, vol. 26, no. 1, pp. 1–11, 2007.

[37] T. Onisawa, "An approach to human reliability in man-machine systems using error possibility," *Fuzzy Sets and Systems*, vol. 27, no. 2, pp. 87–103, 1988.

[38] S. D. Eskesen, P. Tengborg, J. Kampmann, and T. H. Veicherts, "Guidelines for tunnelling risk management: international tunnelling association, working group no. 2," *Tunnelling & Underground Space Technology*, vol. 19, no. 3, pp. 217–237, 2004.